Available online at https://ifejost.oauife.edu.ng

IFE JOURNAL OF SCIENCE AND TECHNOLOGY

Vol 8. No. 1 (2024) 31 – 42

Synthesis, Characterization, Antimalarial Activity and Molecular docking of 2-Oxo-1,2-dihydro-1'*H*-spiro[indoline-3,2'-quinazoline]-4'-carbohydrazones

Omoyeni, O. B.[1], Omisore, N. O. [2], Obafemi, C. A. [1] and Olomola, T. O.[1,*]

[1]Department of Chemistry, Obafemi Awolowo University, Ile-Ife, Nigeria.

[2]Department of Pharmacology, Obafemi Awolowo University, Ile-Ife, Nigeria.

*****Corresponding Author's Email: tolomola@oauife.edu.ng

Abstract

Successfully combating the growing resistance to current antimalarial drugs requires the identification and targeting of essential metabolic pathways in the malaria parasite. In this study, Isatin **1** was used to synthesize isamic ester **2** and its hydrazide **3**, which subsequently led to the development of a series of carbohydrazones (**4**–**14**). The interaction of these carbohydrazones with *Plasmodium falciparum* transketolase (*PfTk*) was evaluated using molecular docking techniques. Among the tested compounds, carbohydrazones **4** and **9** successfully passed pharmacokinetic screening, emerging as lead candidates for antimalarial drug development. *PfTk* plays a crucial role in generating ribose sugars essential for nucleic acid synthesis. In vivo antimalarial chemo-suppression studies using a murine model, with chloroquine and artemether as standards, revealed that compound **9** (10 mg/kg) exhibited activity comparable to chloroquine at the same dosage. Notably, no mortality was observed in test animals 24 days post-administration, suggesting the compound's potential as a *PfTk* inhibitor. The alignment between *in silico* predictions and biological study outcomes further supports this conclusion. Throughout the experiment, 84% of the test animals survived, highlighting the compound's efficacy and low toxicity even at a minimal dose.

Keywords: Isamic ester, Carbohydrazone, Quinazoline, *P. falciparum* transketolase, Antimalarial activity.

INTRODUCTION

Malaria, a life-threatening mosquito-borne disease, affects approximately 500 million people worldwide. Each year, around 250 million cases are reported across 106 countries in Africa, Asia, and Latin America, leading to nearly one million deaths.[1] The emergence of drug resistance in *Plasmodium* species, such as *P. falciparum, P. malariae,* and *P. vivax*, poses a significant challenge in malaria control. Key factors contributing to this resistance include the misuse of antimalarial drugs, reliance on monotherapies, and the prevalence of substandard or counterfeit medicines.[2]

Current malaria chemotherapy relies on various compounds, including quinine, chloroquine, mefloquine, primaquine, artemisinin, and their derivatives. However, the lack of an effective vaccine and the decreasing efficacy of traditional drugs against resistant strains necessitate the search for novel antimalarial agents.[3, 4]

The indole framework plays a crucial role in drug development, forming the backbone of essential biomolecules such as tryptophan and serotonin.[5, 6., 7, 8] Extensive research has revealed its diverse biological activities, including anticancer,[9,10] antimalarial,[11] antimicrobial,[12] analgesic,[13] cardiovascular,[14] antihypertensive,[15] antidiabetic,[16] anti-inflammatory,[17, 18, 19] and anti-HIV[20] properties. Modifying the 3-position of the indole ring with heterocyclic groups has shown promise in developing potent therapeutic compounds.[21, 22, 23, 24, 25, 26, 27]

The Pentose Phosphate Pathway (PPP) is vital for the replication of *Plasmodium* parasites, as it provides ribose sugars necessary for nucleotide and nucleic acid synthesis. A key enzyme in this pathway, transketolase, presents an attractive target for antimalarial drug development. Although its experimental 3D structure is unavailable, homology modeling enables the construction of a reliable structural model for drug discovery efforts.

Isatin (indole-2,3-dione) is a heterocyclic compound with a highly adaptable synthetic structure.[28] It undergoes diverse chemical reactions, including electrophilic substitution, nucleophilic addition, and spiro-annulation,[29] leading to the formation of 2-oxindole derivatives. One of its derivatives, isamic acid (2-oxo-1,2-dihydro-1'H-spiro[indoline-3,2'-quinazoline]-4'-carboxylic acid),[30, 31] exhibits antibacterial properties, making it a promising scaffold for further modification. Isamic acid, composed of oxindole and quinazoline segments linked by a spiro-carbon, exhibits typical carboxylic acidity and is considered a notably weak base. Earlier reports have documented the antibacterial activity of isamic hydrazide and its hydrazones.[32]

This study explores a quinazoline-based endogenous compound as a potential antimalarial agent. It is hypothesized that its lipophilic and endogenous nature could minimize toxicity in humans, while functionalization with polar groups may enhance its medicinal properties. Using computational techniques, we analyze the interactions between our proposed compounds and *P. falciparum* transketolase. The synthesis of 2-oxo-1,2-dihydro-1'H-spiro[indoline-3,2'-quinazoline]-4'-carbohydrazones aims to produce potent enzyme inhibitors that disrupt parasite metabolism. Notably, *P. falciparum* transketolase shares minimal similarity with its human counterpart, potentially reducing off-target effects.

RESULTS AND DISCUSSION

Chemistry

Previous research has reported the reaction of isatin (1) with ammonia in methanol, as illustrated in Scheme 1.[32] Additionally, isamic hydrazide (**3**) and the hydrazone derivatives of various compounds were obtained, with their melting points and percentage yields reported.[32] New compounds (**9**, **10**, and **14**) were synthesized from isamic hydrazide by refluxing compound (**3**) with aromatic aldehydes (ix and x) and ketone (xi) in the presence of 2-3 drops of glacial acetic acid in ethanol in Scheme 2.

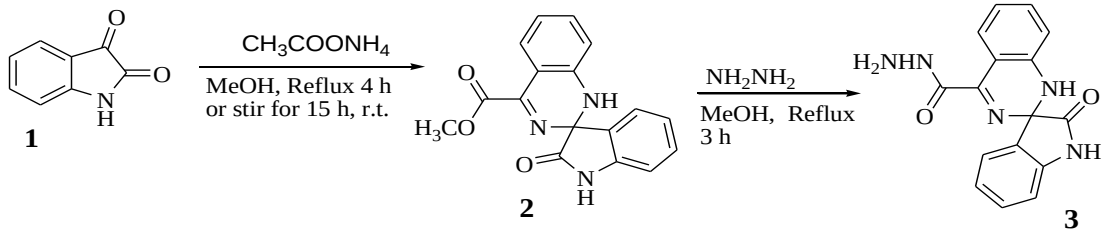

Scheme 1: Synthesis of isamic ester (**2**), hydrazide (**3**) from isatin (**1**)

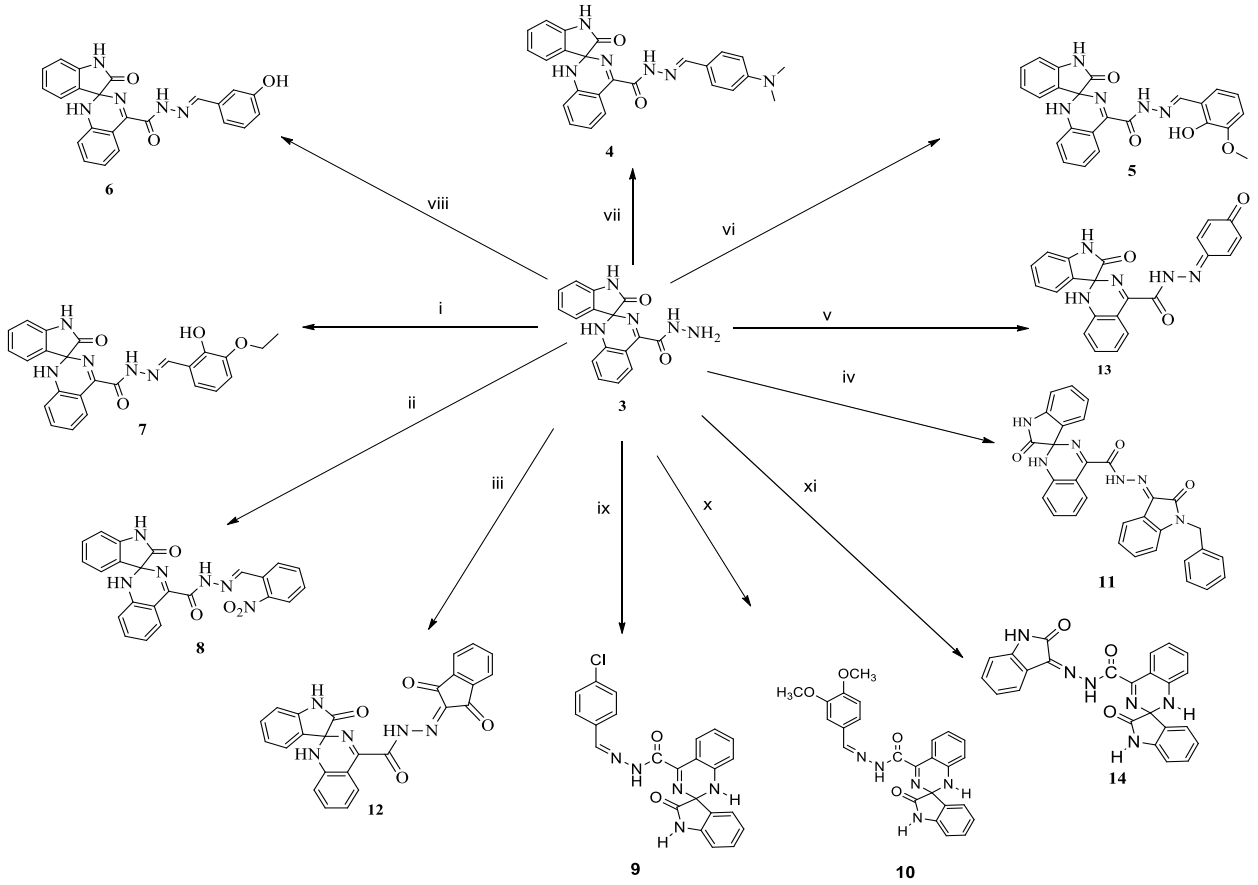

(i) 3-ethoxysalicyaldehyde (ii) 2-nitrobenzaldehyde (iii) ninhydrin (iv) benzylisatin (v) benzoquinone (vi) 3-methoxy-2-hydroxylbenzaldehyde (vii) *para*-dimethylamino benzaldehyde (viii) 3-hydroxylbenzaldehyde (ix) 4-chlorobenzaldehyde (x) 3,4-dimethoxybenzaldehyde (xi) isatin

Scheme 2: Synthesis of 2-oxo-1,2-dihydro-1'*H*-spiro[indoline-3,2'-quinazoline]-4'-carbohydrazones (**4-14**)

The IR, ^{1}H NMR, ^{13}C NMR, and mass spectra of compounds **2-8** and **11-13** have been previously reported.[32] The structures of target compounds **9**, **10**, and **14** were also confirmed through IR, ^{1}H NMR, and ^{13}C NMR analyses. The compounds **9**, **10** and **14** displayed distinctive absorption patterns in their IR spectra. These included peaks at 3362-3421 cm^{-1} indicating the presence of the indolic NH group, 1732-1750 cm^{-1} for the carbonyl C=O group, and 1614 cm^{-1} for the imine C=N group, respectively. The NH proton signals within the indole rings of compounds **9, 10** and **14** were observed between approximately 10.82 and 11.40 ppm in their respective ^{1}H-NMR spectra. In contrast, compounds **9** and **10** showed distinct proton signals (CH=N) from the imine group within the 8.98 to 9.83 ppm region. This observation could be attributed to an interaction between the carbonyl group of the aldehyde's C-H bond and the amino group of isamic hydrazide **3**. Conversely, compound **14** lack identifiable CH=N proton signals due to the absence of a carbonyl-bonded C-H group, being aromatic ketones. The two methoxy protons of compound **10** was observed at 3.82 ppm and 3.84 ppm as singlet. The expected signals were evident in the ^{13}C-NMR spectra of compounds **9, 10** and **14**. For example, signals corresponding to the carbonyl groups were detected within the ppm range of 163.2 to 173.4 ppm. Additionally, the spiro carbons connecting the quinazoline and oxindole segments of compounds **4-14** were detected at approximately 72.1 to 75.8 ppm.

Docking study

Molecular docking provided insight into the interactions and the binding modes of the protein and compounds **4-14**. The active site of the target protein model was determined by visual inspection and superimposition of the templates 3D structure on that protein model. The proteins and the compounds were prepared as described in the experimental section. The 3D structure of compounds (**4-14**) was docked into the target model with the grid box (dimension of the grid box) centered around the active site. The cofactor (TPP) and its synthetic analog (6-methyl TPP) were also docked into the protein to serve as reference. all the compounds **4-14** has the highest binding affinity 7.5-10.5 kcal/mol relative to that of the cofactor (TPP, -7.0 kcal/mol) and synthetic analog (6-methyl TPP, - 7.0 kcal/mol). The higher the binding energy affinity, the stronger the interaction between the protein and the ligand. The resultant binding affinities from all the interactions for the docked compounds are shown in Table 1. This implies that the enzymes have higher affinity for compounds **4-14** relative to that of the cofactor, which suggest that compounds **4-14** has a capacity to displace the cofactor and eventually disrupting the activity of the enzymes, thereby effectively inhibiting the enzyme, and preventing the enzyme from carrying out its catalytic function and subsequently preventing the parasite from carrying out its metabolic activity which will eventually lead to the death of the parasite. This observation was corroborated from a follow up in vivo study using animal model. After conducting docking studies, compounds **4-14** were evaluated for their drug likeness according to Lipinski's rule of five. None of the compounds violated Lipinski's rule of five during the online Pre-ADME studies. Consequently, these compounds were subjected to pharmacokinetic screening. The Lipinski's rule of five is a rule used to determine if a compound with certain pharmacological or biological activity has chemical and physical properties that would make it a likely orally active drug in humans, that is its druglikeness, with reduced toxicity and high bioavailability at the site of action.[33]

Table 1: Binding affinities of the ligands

S/N	Compounds Docked	B.E (kcal/mol)	S/N	Compounds docked	B.E (kcal/mol)
1	**4**	8.1	8	**10**	8.1
2	**5**	8.0	9	**11**	8.8
3	**6**	8.0	10	**12**	8.9
4	**7**	7.9	11	**13**	10.5
5	**8**	7.8	12	**14**	8.3
6	**9**	8.5	13	**SUBTPP**	7.0
7	**Tpp**	7.0			

The online Pre-ADME program was utilized to predict the ADME properties of compounds **4-14**. Their capability to traverse the blood-brain barrier (BBB), CACO-2, MDCK, and human intestinal absorption (HIA) was assessed. Among the eleven compounds (hydrazones), two (**4** and **9**) were identified as inhibitors of P-glycoprotein. Furthermore, these two compounds exhibited high plasma protein binding exceeding 95%. The absorption of all the compounds exceeded 85%, indicating high absorption, and they did not inhibit CYP_2D6. Compounds **4** and **9** exhibited BBB penetration greater than 2, indicating significant absorption into the central nervous system. Compound **4** has a low permeability (values below 25) while compound **9** has a medium permeability (values between 25 to 500). Compounds start to break down as soon as they enter the body. The major family of enzymes associated with these metabolic reactions is the cytochrome P450 family. **4** and **9** (Table 2) were inhibitors of CYP_3A4IN and weakly substrates CYP_3A4SU which makes to be best selected as having the optimum pharmacokinetics properties having passed all the other criterias in the selection.

Table 2: Pharmacokinetics Properties of Compounds 4-14 that Passed the Lipinski's rule

Lig	PgP	Caco2	3A4SU	3A4IN	HIA	MDCK	BBB	PPB
4	inhibitor	17.8128	Weakly	Inhibitor	93.8675	12.6864	2.46539	100
5	Non	19.9864	Weakly	Inhibitor	89.7102	0.051010	0.17823	96.28770
6	Inhibitor	19.0206	Substate	Inhibitor	88.2426	0.046955	0.28854	98.58992
7	Non	20.2362	Weakly	Inhibitor	93.0648	0.271078	0.12352	98.29221
8	Non	18.3975	Weakly	Inhibitor	90.1264	0.051191	0.24523	95.31642
9	Inhibitor	21.7592	Weakly	Inhibitor	94.5621	35.8884	2.31099	95.09783
10	Non	20.0914	Weakly	Inhibitor	89.9265	0.266641	0.29477	100
11	Non	16.4022	Weakly	Inhibitor	93.0441	0.051837	0.03800	73.57016
12	Non	20.34	Substate	Inhibitor	94.3724	0.051410	0.10529	98.70167
13	Non	17.3464	Weakly	Non	89.5643	0.5436	0.10056	68.56437
14	Inhibitor	17.7344	Substate	Inhibitor	95.653	0.046157	0.05286	100

Lig = Ligands, BBB = Blood Brain Barrier Penetration, Pgp = Permeability glycoprotein, HIA = Human Intestinal Absorption MDCK = Madin-Darby canine kidney cell, PPB = Protein Plasma Binding Caco2 = Colorectal adenocarcinomaceas cell. The components highlighted in the study have fulfilled the pharmacokinetics criteria for the antiplasmodial studies.

Figure 1 illustrates a TPP (two-dimensional projection) showcasing residues closely positioned within the binding pocket and participating in various interaction types. It specifically emphasizes the unfavorable positive-positive interaction between Lysine 191 and a positively charged phosphorus, resulting in heightened electrophilicity in the phosphate group. In the SUBTPP representation, the diagram highlights residues in close proximity within the binding pocket, accentuating enhanced electrostatic interactions. The observed docking scores for both compounds **4** and **9** can be ascribed to their multiple interactions with the amino acids present in transketolase. Specifically, compound **4** establishes hydrogen bonds with HIS 71, Pi-cation interactions with HIS 266, ASP 160, and HIS 31, a pi-sigma interaction with LEU 121, and alkyl interactions with ILE 194 and HIS 105. Similar interactions were observed for compound **9** with the amino acids in transketolase, except for the absence of interaction between **9** and HIS 268. The visual representations of these interactions are depicted in Figure 1.

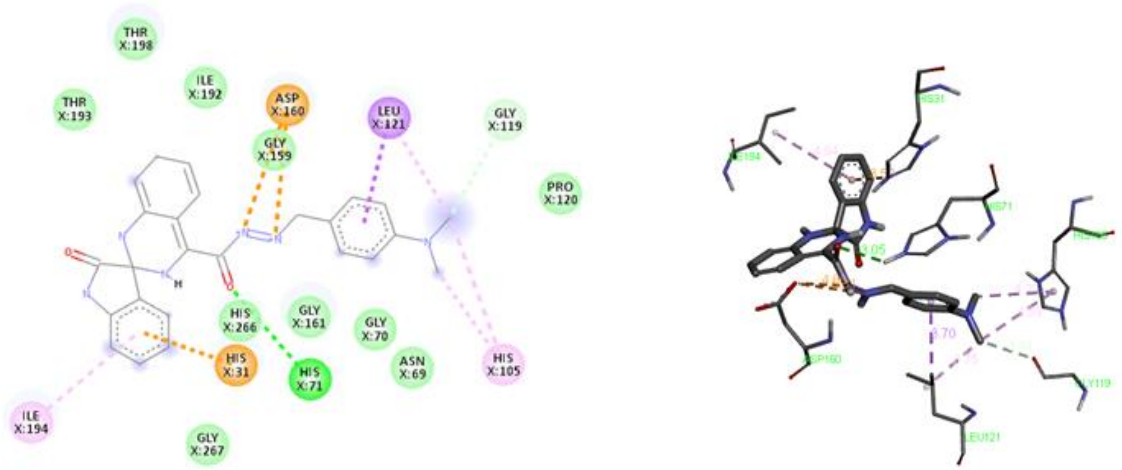

Compound 4

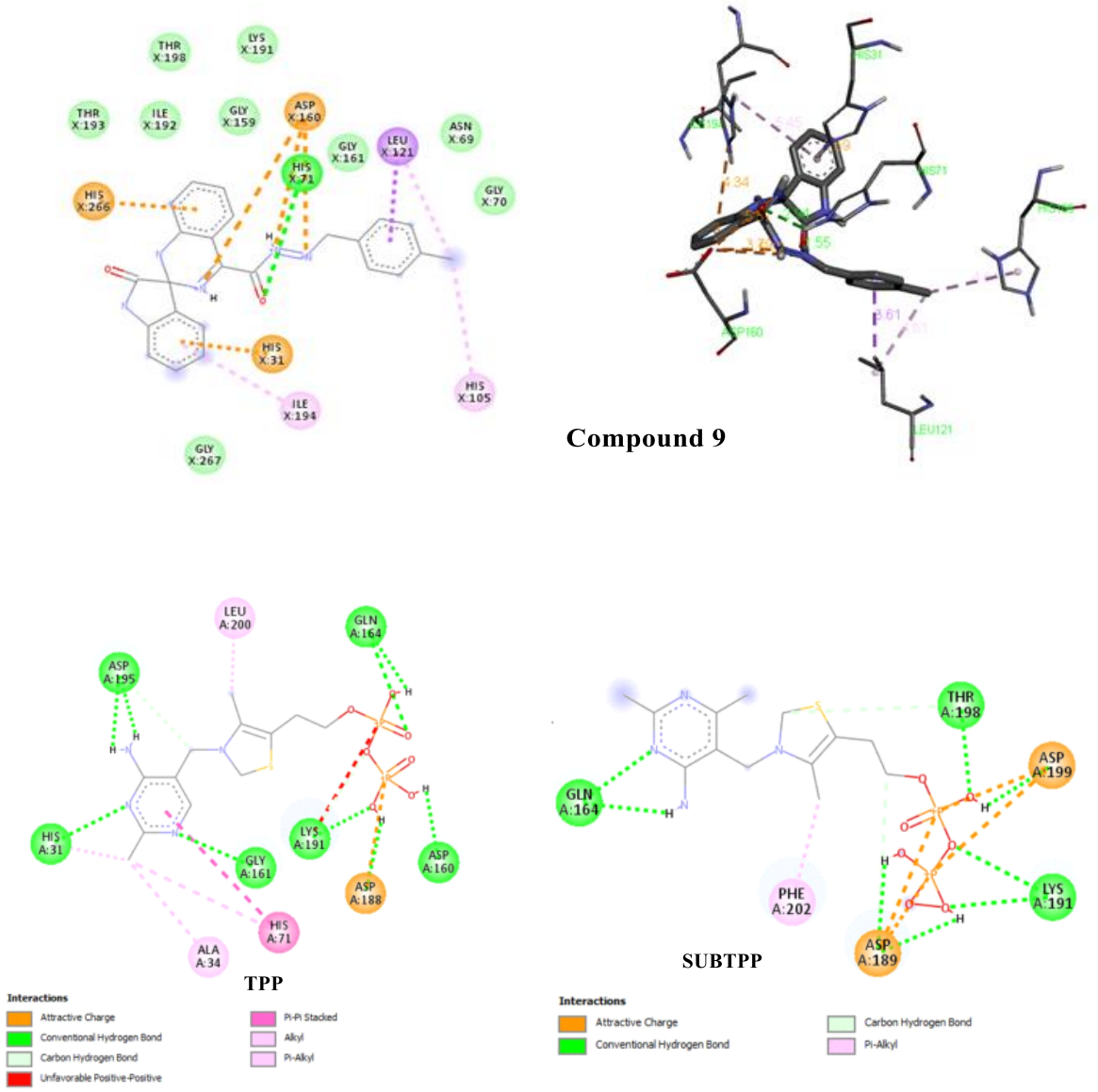

Figure 1: Exploring the Binding Modes of Compound **4** and **9** with Plasmodium Transketolase Inhibitor (*PfTk*): Insights into Interactions with Thiamine Phosphate (TPP) and its Synthetic Analog (SUBTPP)"

In-vivo study

Lethal dose determination

The oral safety of test compounds **4** and **9** was determined through the LD_{50} assay results. Tables 3 and 4 indicated that compound **4** displayed an outstanding safety profile, with no observed mortality rates at any administered dose, including the highest specified dose of 5000 mg/kg, in accordance with OECD guidelines. The substance's dosing advantage becomes evident, with an LD_{50} exceeding 5000 mg/kg having no practical importance. This suggests that compound **4** showed no adverse effects throughout the entire range of dosages. Conversely, compound **9** exhibited a comparatively higher level of toxicity than compound **4**, especially at the dosage of 2154 mg/kg. However, it is essential to emphasize that this sharply contrasts with compound **9** impeccable safety record across all tested doses. Therefore, these findings suggest that compound **9** manifested a heightened degree of toxicity compared to compound **4**.

Table 3: The Median Lethal Dose for Compound 4

Dose (mg/kg)	Number of Animals used	Number of Animals dead	% Mortality
10	3	0	0
100	3	0	0
1000	3	0	0
1600	1	0	0
2900	1	0	0
5000	1	0	0

Table 4: The Median Lethal Dose for Compound 9

Dose (mg/kg)	Number of Animals used	Number of Animals Dead	% Mortality
10	3	0	0
100	3	0	0
1000	3	0	0
1600	1	0	0
2900	1	1	100
5000	1	1	100

LD_{50}= √Least dose of mortality x Highest dose of non-mortality

Therefore, for compound **9**, $LD_{50} = \sqrt{2900 \text{ X } 1600}$ = 2154.07 mg/kg

Antimalarial chemo suppressive test

Compound **4** and **9** demonstrated suppressive antiplasmodial activity based on the assay results. Compound **9** exhibited chemosuppression ranging from 80.93 % to 82.39 % at doses of 5-20 mg/kg, showing good comparison to standard drugs such as chloroquine (10 mg/kg) with 99.28% and more favourably than artemether (25 mg/kg) with 66.20% (Table 5). Conversely, compound **4** displayed chemosuppression ranging from 54.93% to 55.63% at doses of 5-10 mg/kg, with the lowest activity observed at a dose of 20 mg/kg among all the doses used. Compound **9** demonstrated statistically significant values compared to the negative control, whereas compound **4** did not. Therefore, compound **9** exhibits greater activity than compound **4**. However, increasing the doses of compound **4** may result in an increase in its activity (23.94% chemosuppression). Consequently, the parasite faces increased competition. Notably, the highest antimalarial activity was observed in compound **9** at a dosage of 20 mg/kg. Thus, compound **9** shows promise as an alternative for antimalarial drugs

Table 5: Percentage of Parasitaemia Data

Dose (mg /kg)	Mean % Parasitaemia ± SEM	% Chemosuppression	% Survival Rate
0	1.42 ±0.23	0.00	
CQ	0.15 ±0.17	95.85	99.86
ART	0.48 ±0.09	66.20	96.42
4 (5mg/kg)	0.64 ±0.24	54.93	68.75
4 (10mg/kg)	0.63 ±0.13	55.63	60.25
4 (20mg/kg)	1.08 ±0.56	23.94	36.45
9 (5mg/kg)	0.27 ±0.07*	80.93	72.73
9 (10mg/kg)	0.25 ±0.09*	82.39	84.45
9 (20mg/kg)	0.24 ±0.12*	82.39	80.22

*indicates statistical significance

The values obtained for compound **9** were found to be statistically significant to that of the negative control whereas those obtained for **4** were not.

SEM-Standard error mean. CQ = Chloroquine, ART = Artemisinin

Survival index

Compounds, except for compound **4** at a dose of 20 mg/kg in Table 5 showed a significant increase in the survival index in the experimental animals. The experimental animals were monitored for a total of 28 days, consisting of a four-day chemo suppressive test followed by an additional 24-day observation period. The compounds were administered during the initial four days of the assay, and on the fifth day, blood samples were collected from the tails of the experimental animals to perform a thin smear and assess the parasitaemia level (%) in the animals. The % chemosuppression was then calculated using the percentage parasitaemia for the compound relative to that of the negative control. In the same vein, the survival index was estimated as a relative value, measured as the number of days in the experimental animals survived beyond the number of days the negative control survived within 28-day period. At a dosage of 10 mg/kg, compound **9** exhibited the highest level of antimalarial chemosuppression (82.39%) and significantly improved the survival index (84.45%), thus prolonging the lifespan of the animal. The chemosuppressive effect of compound **4** varied from low to moderate, with a decrease in cell viability of 23.94% at 20 mg/kg, 54.93% at 5 mg/kg, and 55.63% at 10 mg/kg. However, the survival index was generally moderate, except for the 20 mg/kg dose, which was considerably low. The standard drug, chloroquine, demonstrated exceptional chemosuppression and survival rates, achieving 99.28% and 99.86% respectively, reported in Table 5.

EXPERIMENTAL SECTION

General methods

The reagents used in this study were obtained from Sigma-Aldrich chemicals, except for ethanol, acetone, ethyl acetate, methanol, n-hexane, and acetic acid, which were acquired from BDH Chemical Limited. Analytical-grade solvents were employed and subjected to purification and drying as needed using standard techniques. Melting points were determined using an open capillary tube on a Gallenkamp variable heater, with no corrections applied to the melting point apparatus. Infrared spectra were captured using an FTIR-8400S Shimazu Spectrometer with KBr pellets. The ^{1}H-NMR and ^{13}C-NMR spectra were acquired at 400 MHz and 100 MHz, respectively, utilizing a Bruker spectrometer (in ppm relative to Me4Si). Mass spectrometry was conducted using a Finnegan Model 4023 instrument, while high-resolution mass spectra were obtained using an Agilent instrument. Column chromatography was performed employing Merck silica gel 60 (230-400 mesh, with a particle size of 0.040-0.063 mm). Thin layer chromatography (TLC) was executed on pre-coated

Merck silica gel F254 plates, observed under UV light. The purity of synthesized compounds was assessed via Thin Layer Chromatography (TLC) on silica gel plates using an n-hexane and ethyl acetate solvent system (3:1, v/v), with developed plates visualized under UV light (254/365 nm).

Synthesis

The synthesis of compounds **2-8** and **11-13**, along with their melting points, colors, and percentage yields, has been previously reported.[32] The synthesis of compounds **9**, **10**, and **14** was conducted by reacting isamic hydrazide (**3**) (6.5 mmol) with ix-xi in ethanol (50 mL). A few drops of glacial acetic acid were added, and the entire reaction mixture was refluxed for approximately 3-4 h. After cooling, the solid that formed was filtered, washed with cold ethanol, and dried in an oven at 50 °C. The product obtained was purified by column chromatography [on silica gel; elution with n-hexane – EtOAc (3:1)], yielding compounds **9**, **10**, and **14**.

.*N*'-(4-chlorobenzylidene)-2-oxo-1'*H*-spiro[indoline-3,2'-quinazoline]-4'-carbohydrazide 9

Orange solid (yield 1.78 g, 64%); m.p 285-287 ^{o}C; IR (KBr, cm^{-1}) 3362, (NH) 3019 (sp^{2}C-H), 1732, 1699 (C=O), 1614 (C=N), 1591, 1465 (C=C) Ar, 1500 (N-H bending), 740; δ_H (400 MHz; DMSO-d_6) 6.43 (1H, s, ArH), 7.05 (1H, dd, *J* = 7.3, 1.6 Hz, ArH), 7.10-7.23 (5H, m, ArH), 7.33–7.41 (4H, m, ArH), 7.58 (1H, dd, *J* = 7.3, 1.6 Hz, ArH), 7.80 (1H., dd, *J* = 7.3, 1.6 Hz, ArH), 8.98 (1H, s, CHN), 11.40 (1H, s, NHCO); δ_C (100 MHz; DMSO-d_6) 72.1 (spiro C), 110.3, 111.8, 112.7, 114.9, 118.3, 121.2, 121.2, 126.8, 127.0, 129.5, 133.0, 135.2, 135.2, 136.6, 137.9, 138.5, 139.9, 140.9 146.9 (Ar-H), 157.3 (C=N), 166.3 and 169.3(C=O).

***N'*-(3,4-Dimethoxybenzylidene)-2-oxo-1'*H*-spiro[indoline-3,2'-quinazoline]-4-carrbohydrazide 10**

Orange solid (yield 2.02 g, 68%), m.p 291-293 ^{o}C; IR (KBr, cm^{-1}) 3362, (NH) 3019 (sp^2 C-H), 1732, 1699 (C=O), 1614 (C=N), 1591, 1465 (C=C) Ar; δ_H (400 MHz, DMSO-d_6) 3.82 (3H, s, OCH_3), 3.84 (3H, s, OCH_3), 6.33 (1H, s, NH), 6.98 (2H, dd, *J* =7.3, 1.6 Hz, ArH), 7.09–7.26 (4H, m, ArH), 7.43 (1H, d, *J* = 1.5 Hz, ArH), 7.55 (1H, dd, *J* = 7.3, 1.6 Hz, ArH), 7.68 (1H, dd, *J*= 7.5, 1.6 Hz, ArH), 7.81 (1H, d, *J* = 1.5 Hz, ArH), 8.03 (1H, s, ArH), 9.83 (1H, s, CHN), 11.17 (1H, s, NHCO); δ_C (100 MHz, DMSO- d_6) 55.9 and 56.3 (OCH_3), 75. 8 (spiro C), 110.1, 110.4, 111.7, 117.3, 117.9, 121.5, 121.8, 122.7, 123.2, 126.7, 127.5, 128.9, 129.1, 130.7, 139.1, 140.9, 146.3, 149.5, 149.9 (CHN), 151.4 (C=N), 163.2 and 166.6 (C=O).

***N'*-(2-Oxoindolin-3-ylidene)-2-oxo-1'*H*-spiro[indoline-3,2'-quinazoline]-4'-carbohydrazide 14**

Reddish brown solid (yield 1.88 g, 66%), m.p. 285-287; IR (KBr, cm^{-1}) 3421 (NH), 3080 (sp^2-CH), 1752, 1712 and 1693 (C=O), 1610 (C=N); δ_H (400 MHz, DMSO) 6.53 (1H, s, NH), 7.05 (1H, dd, *J* = 7.4, 2.0 Hz, ArH), 7.10-7.17 (2H, m, ArH), 7.17-7.23 (3H, m, ArH), 7.26 (1H, td, *J* = 7.3, 1.7 Hz, ArH), 7.31-7.41 (2H, m, ArH), 7.58 (1H, dd, *J* = 7.4, 2.0 Hz, 1H), 7.75 (1H, s, ArH), 7.91 (2H, ddd, *J* = 7.3, 4.5, 1.7 Hz, ArH), 10.82 (1H, 1s, NHCO); δ_C (100 MHz, DMSO- d_6) 75.5, 113.1, 113.8, 116.7, 119.6, 121.5, 122.45, 122.48, 123.4, 125.1, 127.3, 127.7, 128.6, 128.58, 128.90, 131.6, 136.9, 139.6, 141.2,147.5 (Ar-C), 147.5 (C=N), 162.7, 165.3 and 173.4 (C=O).

Molecular docking

The docking studies were carried out using Autodock tools v1.5.4.[34] Autodock Vina v1.1.2.[35] The protein (*plasmodium falciparum* transketolase *PfTk*) used was obtained.[33] The Chemical structures were drawn using Chemdraw v12.0, and energy minimization was achieved through Chem 3D v12.0. The molecular docking process involved the carbohydrazone derivatives (**4-14**), thiamine pyrophosphate (TPP), and 6-methyl thiamine pyrophosphate (SUBTTP) using Autodock tools. Both TPP, recognized as a coenzyme in transketolase, and 6-methyl TPP (SUBTPP) were utilized as reference compounds throughout this procedure. The protein was transformed from .pdb to. pdbqt format before its binding site was analyzed and marked as a grid box (search space area) through the

application of the AutoDOCK tool. To prepare the ligands for docking, Chem3D and AutoDock Tools were employed. After the preparation of both the ligands and protein, each specific ligand was docked into the protein using AutoDock Vina. This process aimed to assess the binding affinity and identify the most favorable binding pose.

BIOLOGICAL STUDY

Lethal dose determination

The acute toxicity of compound **4** and **9** was determined using Lorke's method.[36] The experiment consisted of two phases. During the first phase, three groups, each containing three mice, were utilized. The ligands were administered to each group at doses of 10, 100, and 1000 mg/kg, and the mice were observed for mortality over a period of 24 hours. Positive results from phase one determined the continuation to phase two. In the second phase, another set of three groups, each with one mouse (n=1), was employed. The ligands were administered at doses of 1600, 2900, and 5000 mg/kg to these groups, and the mice were again observed for mortality for 24 hours.

Antimalarial chemo suppressive test

Groups of five Swiss white mice were partitioned, and each group was subjected to intraperitoneal inoculation with 1.0 x 10^7 *P. bergheli* parasites. Various concentrations of compounds **4** and **9** were dissolved in a 1:1 mixture of DMSO and water. Three groups received oral doses of the compound at 5, 10, and 20 mg/kg, respectively. Meanwhile, two additional groups were subjected to administration of 10 mg/kg chloroquine and 25 mg/kg artemether (reference drugs), and 0.2 mL of the preparation vehicle (negative control), respectively. The test agents were administered for four (4) consecutive days. On the fifth day, thin blood smear was prepared and the blood films were stained with Giemsa solution and then microscopically examined with 100 x magnification (oil immersion). The percentage chemo suppression of parasitaemia was calculated for each dose level by comparing the % parasitaemia of the controls with those treated mice.[37] The percentage parasitaemia of the experimental animals after the four days of drug administration was estimated as count of parasitized red blood cells divided by the total red blood cells counted within microscopic fields. The percentage chemo suppression (Table 5.0) was calculated as a relative value taking into account the % parasitaemia of the negative control. The formula used is as described below

$$\% \text{ Parasitaemia} = \frac{\text{Total number of PRBC}}{\text{Total number of RBC}} \text{ x } 100\%$$

PRBC = parasitized red blood cells, RBC = red blood cells

$$\textbf{\%} \text{ Chemosuppression} = \frac{\text{Parasitaemia in control} - \text{Parasitaemia in test}}{\text{Mean \% parasitaemia in control}} \text{ x } 100\%$$

Statistical analysis

The parasitaemia was determined to find quantitatively the presence and degree of activity at the screening doses. One-way ANOVA with student –Newman keul's test was used. Statistical significance we set at $p < 0.05$. the results were expressed as Mean ± SEM (Standard error of mean).

Survival index

The survival indices of the experimental animals for each of the test compounds are presented as a relative value (in percentage) taking into consideration the survival time of the negative control group of animals and the survival time of the experimental animals. The survival indices (in percentage) of the experimental drugs were calculated using the formula shown in equation below.

$$\text{Survival index (\%)} = \frac{(A-B)}{(28-B)} \text{ x } 100\%$$

where A = Last day of animal with test drug and B = Last day of animal without drug (negative control).

CONCLUSION

In summary, Isamic ester **2** and its hydrazide **3** were sequentially synthesized from isatin **1** as intermediates. A series of novel carbohydrazones were then derived from the hydrazide of Isamic ester **2**.

In the in-silico studies, eleven ligands (**4**–**14**) were docked with a modelled protein using AutoDock Vina, and their binding energies were determined and analysed for pharmacokinetic properties. Among them, compounds **4** and **9** exhibited the most favourable profiles and were selected for in-vivo evaluation.

Subsequent in-vivo studies confirmed the antimalarial activity of compound **9** at a minimum effective dose of 10 mg/kg, with an 84% survival rate among test animals, indicating both efficacy and low toxicity.

These findings highlight the potential of these chemical groups as promising candidates for combating drug-resistant malaria, warranting further investigation.

REFERENCES

[1] World Health Organization (WHO). http://www.who.int/features/factfiles/malaria/en/index.html/ (accessed on 10 March 2011).

[2] World Health Organization (WHO). Global report on antimalarial drug efficacy and drug resistance: 2000–2010. Available online: http://www.who.int/malaria/en (accessed on 10 March 2011).

[3] Kaur, K.; Jain, M.; Reddy, R.P.; Jain, R. *Eur. J. Med. Chem*. 2010, 45, 3245-3264.

[4] Biot, C.; Chibale, K. *Infect. Disord*. -Drug Targets 2006, 6, 173-204.

[5] M. Shiri, *Chem. Rev*. 112 (2012) 3508–3549.

[6] J.J. Song, J.T. Reeves, D.R. Fandrick, Z. Tan, N.K. Yee, C.H, *Arkivoc* 1 (2010) 390–449.

[7] D. Zhang, H. Song, Y. Qin, *Acc. Chem. Res*. 44 (2011) 447–457.

[8] S. Ke, L. Shi, X. Cao, Q. Yang, Y. Liang, Z. Yang, *Eur. J. Med. Chem*. 54 (2012) 248–254.

[9] C.M. Cover, S.J. Hsieh, E.J. Cram, C. Hong, J.E. Riby, L.F. Bjeldanes, G.L. Firestone, *Cancer Res*. 59 (1999) 1244–1251.

[10] V.R. Solomon, C. Hua, H. Lee, Bioorg. *Med. Chem*. 18 (2010) 1563–1572.

[11] Chiyanzu, C. Clarkson, P.J. Smith, J. Lehman, J. Gut, P.J. Rosenthal, K. Chibale. *Bioorg. Med. Chem*. 13 (2005) 3249–3261.

[12] A. Scribner, J.A. Moore, G. Ouvry, M. Fisher, M. Wyvratt, P. Leavitt, P. Liberator, A. Gurnett, C. Brown, J. Mathew, D. Thompson, D. Schmatz, T. Biftu, *Bioorg. Med. Chem. Lett.* 19 (2009) 1517–1521.

[13] M.A.A. Radwan, E.A. Ragab, N.M. Sabry, S.M. El-Shenawy, Bioorg. Med. Chem. 15 (2007) 3832–3841.

[14] A. Kumar, K.K. Saxena, S. Gurtu, J.N. Sinha, K. Shanker, *Indian Drugs* 24 (1986) 1–5.

[15] H.S. Kim, Y. Kim, M.R. Doddareddy, S.H. Seo, H. Rhim, J. Tae, A.N. Pae, H. Choo, Y.S. Cho, *Bioorg. Med. Chem. Lett.* 17 (2007) 476–481.

[16] Y. Lamotte, P. Martres, N. Faucher, A. Laroze, D. Grillot, N. Ancellin, Y. Saintillan, V. Beneton, R.T. Gampe, Bioorg. *Med. Chem*. Lett. 20 (2010) 1399–1404.

[17] K.R. Abdellatif, P.F. Lamie, H.A. Omar, *J. Enzyme Inhib. Med. Chem. 31* (2016) 318–324.

[18] F.L. Phoebe, A.M.A. Waleed, B. Vaclav, R. Lucie, *Eur. J. Med. Chem*. 123 (2016) 803–813.

[19] M.Y. Ebeid, S.M. Lashine, S.M. El-Adl, M.E. Abou Kull, *Zagazig J. Pharmaceut. Sci*. 3 (1994) 40–48.

[20] L. Chiummiento, M. Funicello, P. Lupattelli, F. Tramutola, P. Campaner, *Tetrahedron* 65 (2009) 5984–5989.

[21] Y. Boursereau, I. Coldham, *Bioorg. Med. Chem. Lett*. 14 (2004) 5841–5844.

[22] Nagendra Kumar Kaushik, NehaKaushik, PankajAttri, Naresh Kumar, Chung Hyeok Kim, Akhilesh Kumar Verma, Eun Ha Choi, *Molecules* 18 (2013) 6620–6662.

[23] S.B. Singh, D.L. Zink, J.D. Polishook, A.W. Dombrowski, S.J. Darkin-Rattray, D.M. Schmatz, M.A. Goetz, *Tetrahedron Lett.* 37 (1996) 8077–8080.
[24] P.T. Meinke, S.L. Colletti, M.B. Ayer, S.J. Darkin-Rattray, R.W. Myers, D.M. Schmatz, M.J. Wyvratt, M.H. Fisher, *Tetrahedron Lett.* 41 (2000) 7831–7835.
[25] S.L. Colletti, R.W. Myers, S.J. Darkin-Rattray, A.M. Gurnett, P.M. Dulski, S. Galuska, J.J. Allocco, M.B. Ayer, C. Li, *Bioorg. Med. Chem. Lett*. 11 (2001) 113–117.
[26] L.F. Tietze, *Chem. Rev*. 96 (1996) 115–136.
[27] A. Domling, Recent developments in isocyanide based multicomponent reactions in applied chemistry, *Chem. Rev*. 106 (2006) 17–89.
[28] Chowdhary, S., Shalini, Arora, A. and Kumar, V. *Pharmaceuticals*, 15(5), 536.
[29] Da Silva, J. F., Garden, S. J., & Pinto, A. C. *Journal of the Brazilian Chemical Society*, 12, 273-324.
[30] Mayo, P. D, & Ryan, J. J. *Canadian Journal of Chemistry*, 45(19), 2177-2190.
[31] Bergman, J., Arewang, C. J., & Svensson, P. H. *The Journal of Organic Chemistry*, 79(19), 9065-9073.
[32] Omoyeni, O. B., Omisore, N. O., Obafemi, C. A., and Olomola, T. O. *Chemistry Select*, 9(17), e202400433.
[33] Fadare O.A., Omisore, O.N., Adegbite, O.B., Awofisayo, O.A., Ogundolie, F.A., Adesanwo, J.K., Obafemi, C.A.
[34] Morris, G. M., Huey, R., Lindstrom, W., Sanner, M. F., Belew, R. K., Goodsell, D. S., and Olson, A. J. *Journal of computational chemistry*, 30(16), 2785-2791.
[35] Trott, O., and Olson, A. J. (2010). AutoDock Vina: *Journal of computational chemistry*, 31(2), 455-461.
[36] Lorke, D. *Archives of toxicology*, 54, 275-287.
[37] Knight, D. J., & Peters, *Annals of Tropical Medicine & Parasitology*, 74(4), 393-404.